Available online at www.sciencedirect.com
ScienceDirect
Journal of Sound and Vibration 304 (2007) 987–995
JOURNAL OF SOUND AND VIBRATION
www.elsevier.com/locate/jsvi

Short Communication

Semi-analytical solutions for free vibration of anisotropic laminated plates in cylindrical bending

C.F. Lü*, Z.Y. Huang, W.Q. Chen

Department of Civil Engineering, Zhejiang University, Hangzhou 310027, PR China

Received 26 December 2006; received in revised form 7 March 2007; accepted 10 March 2007
Available online 4 May 2007

Abstract

Elasticity solutions for free vibration of angle-ply laminates subjected to cylindrical bending are obtained using a newly developed semi-analytical approach. The thickness domain is solved analytically using the transfer matrix method based on the state space concept, while the in-plane domain is solved approximately via the technique of differential quadrature. The present method is applicable to arbitrarily thick laminates and for treating arbitrary edge conditions. The method is verified by comparisons with the exact solutions of Pagano's problem. Effects of variation of ply angle on the vibration properties of laminates are investigated; mode shape switching is observed when ply angle varies. Numerical results for fully clamped thick laminates are presented for future references.

1. Introduction

When it comes to the cylindrical bending of composite laminated plates, two exact elasticity solutions respectively for cross-ply and anisotropic angle-ply laminated plates presented by Pagano [1,2] were always adopted as the benchmark references. It is obvious that the former is a case of plane strain problem, while the latter concerns three-dimensional (3D) issues. These two problems are commonly referred as the Pagano's problem. Most recently, Chen and Lee [3] presented the 3D exact analysis of angle-ply laminates in cylindrical bending using the state space approach (SSA). The difference from Pagano's problem lies in that all laminas are assumed bonded imperfectly at the adjacent interfaces. All these exact solutions are limited to the plates with two edges simply supported. Several generalized higher-order two-dimensional (2D) simplified theories were proposed to investigate static bending [4] and free vibration [5,6] of angle-ply laminates in cylindrical bending. However, numerical results presented in Refs. [5,6] were again only for fully simply supported conditions.

Differential quadrature method (DQM), a numerical technique for solving differential equations proposed by Bellman and his associates in the early 1970s [7,8], has been approved to be highly efficient for obtaining numerical solutions of boundary/initial problems [9,10]. It was recently introduced to the state space formalism by Chen et al. [11,12] to derive semi-analytical 2D elasticity solutions for laminated beams. This

*Corresponding author. Tel.: +86 571 87952284; fax: +86 571 87952165.
E-mail address: lucf@zju.edu.cn (C.F. Lü).

0022-460X/$ - see front matter © 2007 Elsevier Ltd. All rights reserved.
doi:10.1016/j.jsv.2007.03.023

hybrid method, termed as the state-space-based differential quadrature (SSDQM), allows the edge boundary conditions to be treated precisely at each point along the thickness direction so that the Saint–Venant principle becomes unnecessary. It was subsequently applied by Chen and Lee [13] to free vibration analysis of cross-ply laminates in cylindrical bending with arbitrary boundary conditions; the plates under investigation are exactly in the state of plane strain. In the present paper, the hybrid method of SSDQM is employed to obtain semi-analytical 3D elasticity solutions for free vibration of anisotropic angle-ply laminates in cylindrical bending with different sets of edge boundary conditions. Numerical results, especially for strongly thick laminates with non-fully simply supported edges, are presented and believed of adequate accuracy for the reference of future numerical analyses.

2. Semi-analytical formulations

2.1. State-space equation via differential quadrature rule

Consider an m-layered angle-ply laminates (see Fig. 1) in cylindrical bending along the y-coordinate, that is, all variables are independent of the coordinate y. The Cartesian coordinate system is established so that $0 \leqslant x \leqslant l$ and $0 \leqslant z \leqslant h$, as shown in Fig. 1(a), while the material fibers are assumed to orient at an angle θ about the x-coordinate shown in Fig. 1(b).

Assuming that the laminates is in the state of harmonic motion, the set of first-order simultaneous differential equations of state variables, at an arbitrary point in the kth layer ($1 \leqslant k \leqslant m$), with respect to the thickness coordinate z can then be derived as [3]

$$\frac{\partial}{\partial z}\begin{Bmatrix}\sigma_z\\ u\\ v\\ w\\ \tau_{xz}\\ \tau_{yz}\end{Bmatrix} = \begin{bmatrix} & \mathbf{0} & & -\rho\omega^2 & -\frac{\partial}{\partial x} & 0\\ & & & -\frac{\partial}{\partial x} & c_7 & c_8\\ & & & 0 & c_8 & c_9\\ c_{10} & c_4\frac{\partial}{\partial x} & b_3\frac{\partial}{\partial x} & & & \\ c_4\frac{\partial}{\partial x} & -\rho\omega^2 - c_1\frac{\partial^2}{\partial x^2} & -b_1\frac{\partial^2}{\partial x^2} & & \mathbf{0} & \\ b_3\frac{\partial}{\partial x} & -b_1\frac{\partial^2}{\partial x^2} & -\rho\omega^2 - c_6\frac{\partial^2}{\partial x^2} & & & \end{bmatrix}\begin{Bmatrix}\sigma_z\\ u\\ v\\ w\\ \tau_{xz}\\ \tau_{yz}\end{Bmatrix}, \tag{1}$$

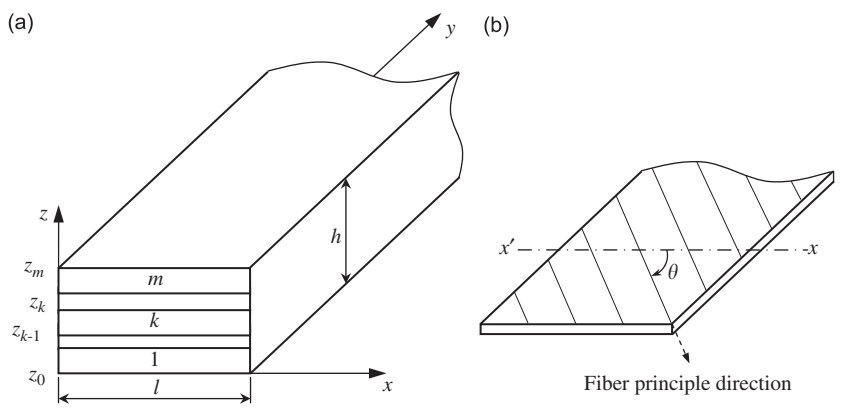

Fig. 1. Geometry and coordinate system of an angle-ply laminates in cylindrical bending: (a) a laminates in cylindrical bending; and (b) laminate scheme of a typical layer.

where ρ is the mass density and ω the circular frequency. All displacement and stress components in Eq. (1) are called the state variables, while the accompanied induced variables are given by

$$\begin{Bmatrix} \sigma_x \\ \sigma_y \\ \tau_{xy} \end{Bmatrix} = \begin{bmatrix} -c_4 & c_1\dfrac{\partial}{\partial x} & b_1\dfrac{\partial}{\partial x} \\ -c_5 & c_3\dfrac{\partial}{\partial x} & b_2\dfrac{\partial}{\partial x} \\ -b_3 & b_1\dfrac{\partial}{\partial x} & c_6\dfrac{\partial}{\partial x} \end{bmatrix} \begin{Bmatrix} \sigma_z \\ u \\ v \end{Bmatrix}. \tag{2}$$

In the above two equations, the coefficients c_i and b_j are determined by the stiffness constants of constitutive relations and are given in Appendix A. It is noted that Eq. (1) reduces to the state equation governing the plane strain problem when $\theta = 0^\circ$ or 90° [13].

For such a plate with two edges simply supported, an exact solution can be obtained by expanding the state variables into trigonometric series about coordinate x [3]. However, if the laminates subject to edge constrained conditions other than simple supports, say clamped or free, it is rather difficult to seek for an exact or analytical solution to Eq. (1). A semi-analytical solution using the technique of differential quadrature was recently proposed by Chen et al. [11,12] for laminated beams, and was subsequently applied to plane strain problem of laminated plates in cylindrical bending [13]. Applying the routine procedure of differential quadrature [14] to Eq. (1), the following state equation at an arbitrary discrete point x_i ($i = 1, 2, \ldots, N$) is straightforward:

$$\begin{aligned}
\frac{\mathrm{d}\sigma_{z,i}}{\mathrm{d}z} &= -\rho\omega^2 w_i - \sum_{k=1}^{N} g_{ik}^{(1)} \tau_{xz,k}, \\
\frac{\mathrm{d}u_i}{\mathrm{d}z} &= -\sum_{k=1}^{N} g_{ik}^{(1)} w_k + c_7 \tau_{xz,i} + c_8 \tau_{yz,i}, \\
\frac{\mathrm{d}v_i}{\mathrm{d}z} &= c_8 \tau_{xz,i} + c_9 \tau_{yz,i}, \\
\frac{\mathrm{d}w_i}{\mathrm{d}z} &= c_{10} \tau_{xz,i} + c_4 \sum_{k=1}^{N} g_{ik}^{(1)} u_k + b_3 \sum_{k=1}^{N} g_{ik}^{(1)} v_k, \\
\frac{\mathrm{d}\tau_{xz,i}}{\mathrm{d}z} &= c_4 \sum_{k=1}^{N} g_{ik}^{(1)} \sigma_{z,k} - \rho\omega^2 u_i - c_1 \sum_{k=1}^{N} g_{ik}^{(2)} u_k - b_1 \sum_{k=1}^{N} g_{ik}^{(2)} v_k, \\
\frac{\mathrm{d}\tau_{yz,i}}{\mathrm{d}z} &= b_3 \sum_{k=1}^{N} g_{ik}^{(1)} \sigma_{z,k} - b_1 \sum_{k=1}^{N} g_{ik}^{(2)} u_k - \rho\omega^2 v_i - c_6 \sum_{k=1}^{N} g_{ik}^{(2)} v_k,
\end{aligned} \tag{3}$$

where N is the total discrete point number along the x direction, and $g_{ik}^{(n)}$ are the weighting coefficients of the differential quadrature rule for the nth-order derivatives [14]. Similarly, the induced variables at the discrete point x_i can be obtained as

$$\begin{aligned}
\sigma_{x,i} &= -c_4 \sigma_{z,i} + c_1 \sum_{k=1}^{N} g_{ik}^{(1)} u_k + b_1 \sum_{k=1}^{N} g_{ik}^{(1)} v_k, \\
\sigma_{y,i} &= -c_5 \sigma_{z,i} + c_3 \sum_{k=1}^{N} g_{ik}^{(1)} u_k + b_2 \sum_{k=1}^{N} g_{ik}^{(1)} v_k, \\
\tau_{xy,i} &= -b_3 \sigma_{z,i} + b_1 \sum_{k=1}^{N} g_{ik}^{(1)} u_k + c_6 \sum_{k=1}^{N} g_{ik}^{(1)} v_k.
\end{aligned} \tag{4}$$

In the above two equations, x_i are coordinates of sampling points, determined, in the current work, by the Chebyshev-Gauss-Lobatto points in cosine pattern [15] as

$$x_i = \frac{l}{2}\left[1 - \cos\frac{(i-1)\pi}{N-1}\right], \quad i = 1, 2, \ldots, N. \tag{5}$$

2.2. Boundary conditions and solutions

In order to achieve a unique solution for a practical problem, the edge-constrained conditions should be incorporated into the state equation, Eq. (3). To illustrate the application of SSDQM in this paper, only simple supports and clamped edge constraints are considered. They are expressed in terms of displacement and stress components as: simply supported edge (S) with $\sigma_{x,i} = \tau_{xy,i} = w_i = 0$; and clamped edges (C) with $u_i = v_i = w_i = 0$, where $i = 1$ or $i = N$. Note that, for the simply supported edge, some of the constrained conditions are expressed in terms of the induced variables. For the purpose of analysis, these conditions should be re-expressed by state variables according to Eq. (4). Detailed procedure of handling boundary conditions can be found in Ref. [13], and, for brevity, is not repeated here. Taking account of all boundary conditions into state equation, Eq. (3), and assembling all the state equations at discrete points lead to the global state equation for the kth layer as follows:

$$\frac{\mathrm{d}}{\mathrm{d}z}\boldsymbol{\delta}^{(k)}(z) = \mathbf{A}_k\boldsymbol{\delta}^{(k)}(z), \tag{6}$$

where $\boldsymbol{\delta}^{\mathrm{T}} = [\,\boldsymbol{\sigma}_z^{\mathrm{T}} \quad \mathbf{u}^{\mathrm{T}} \quad \mathbf{v}^{\mathrm{T}} \quad \mathbf{w}^{\mathrm{T}} \quad \boldsymbol{\tau}_{xz}^{\mathrm{T}} \quad \boldsymbol{\tau}_{yz}^{\mathrm{T}}\,]$ is the global state vector composed of state variables at all discrete points, and $\mathbf{A}_k$ is the coefficient matrix for the kth layer obtained from Eq. (3) by considering all edge constrained conditions. The explicit expression of matrix $\mathbf{A}_k$ is omitted here for simplicity.

For the case of homogeneous plate, the general solution of Eq. (6) is

$$\boldsymbol{\delta}^{(k)}(z) = \mathbf{T}_k(z)\boldsymbol{\delta}^{(k)}(z_{k-1}) \quad (z_{k-1} \leqslant z \leqslant z_k), \tag{7}$$

for $k = 1, 2, \ldots, m$, where $\mathbf{T}_k(z) = \exp[(z - z_{k-1})\mathbf{A}_k]$ is the transfer matrix, through which the state vector $\boldsymbol{\delta}^{(k)}(z_{k-1})$ at the bottom surface of the kth layer is transferred to that at an arbitrary coordinate z. According to the treatment of laminated beams [11,12], a global transfer relation for the present angle-ply plate can be derived by connecting solutions for all layers through appropriate continuity conditions at interfaces as

$$\boldsymbol{\delta}^{(m)}(h) = \mathbf{T}\boldsymbol{\delta}^{(1)}(0), \tag{8}$$

where $\mathbf{T} = \mathbf{T}_m\mathbf{T}_{m-1}\ldots\mathbf{T}_2\mathbf{T}_1$ is called the global transfer matrix. It should be pointed out that, for the sake of numerical stability, joint coupling matrices [16] would be used by decomposing the laminates into several sub-layers, similar to the way for the analysis of continuous Kirchhoff plates [17].

For free vibration, the lateral surfaces are tractions free, that is, all the stress components contained in Eq. (8) equal to zero, and, hence, non-trivial solution of this problem leads to the frequency equation as follows:

$$\begin{vmatrix} \mathbf{t}_{12} & \mathbf{t}_{13} & \mathbf{t}_{14} \\ \mathbf{t}_{52} & \mathbf{t}_{53} & \mathbf{t}_{54} \\ \mathbf{t}_{62} & \mathbf{t}_{63} & \mathbf{t}_{64} \end{vmatrix} = 0, \tag{9}$$

in which $\mathbf{t}_{ij}$ is the partitioned matrices of matrix $\mathbf{T}$. After obtaining natural frequencies from Eq. (9), the normal modes of plates at the bottom surface can be obtained by substituting frequencies into Eq. (8) accompanied with surface tractions boundary conditions. After that, repeat application of general solution, Eq. (7) yields the global state vector at arbitrary coordinate z according to special requests.

3. Numerical examples

Several numerical examples are performed to validate the present method for 3D analysis of anisotropic laminates subjected to cylindrical bending. The edge conditions of plates in consideration are of simply–simply (SS) and clamped–clamped (CC) constraints. Material properties are selected according to Pagano's work [2], i.e.

$$E_L/E_T = 25, \quad G_{LT}/E_T = 0.5, \quad G_{TT}/E_T = 0.2, \quad v_{LT} = v_{LT} = 0.25,$$

where E, G and v are, respectively, the Young's modulus, shear modulus and Poisson's ratio, and subscripts L and T represent the direction parallel and perpendicular to material fiber, respectively. All layers of plates are assumed of the same thickness, i.e. $h_k = h/m$ ($k = 1, 2, \ldots, m$). For the sake of comparison, numerical results of natural frequencies are presented in the normalized form of $\bar{\omega} = \omega h\sqrt{\rho/G_{LT}}$.

Firstly, an angle-ply laminated SS plate with the aspect ratio of $h/l = 0.1$ is considered. The plate is composed of different number of layers with the lamina scheme of $45^\circ/-45^\circ/\ldots$, which includes symmetric and antisymmetric cases. Fundamental frequency parameters are computed using SSDQM for different sampling point numbers, and compared to that obtained from 2D higher order theories [5] as well as exact 3D elasticity solutions by expanding all variables into trigonometric series [3]. The results are listed in Table 1 in conjunction with the relative percentage error $e\% = (\bar{\omega} - \bar{\omega}_0)/\bar{\omega}_0 \times 100\%$ against the exact results $\bar{\omega}_0$. It is satisfactory to notice that, regardless of layers arrangement, frequency parameters converge rapidly to the 3D exact results as N increases. Results following M2D are obtained based on the generalized mixed-based plate theory [5] and the followed number indicates the terms associated with higher-order displacement and shear stresses involved in the theory. The current results when $N = 7$ achieve similar accuracy to that of M2D-11 for the fundamental frequencies. When $N = 9$, the present results deviated form 3D exact solutions with extremely small relative errors having an order of only 10^{-4}. Table 2 exhibits that the present method converges rapidly and is highly accurate for predicting fundamental frequency parameters of strongly thick laminates with $h/l = 0.3$ and 0.4.

To further validate convergence properties of SSDQM, frequency parameters $\bar{\omega}$ of CC plates are computed. Table 3 lists fundamental frequencies of CC plates having the same aspect ratio and layers arrangement as that in Table 1, while Table 4 presents the first six frequency parameters of a thick CC plate ($h/l = 0.25$) with

Table 1
Fundamental frequency parameters $\bar{\omega}$ of SS plates composed of different layer numbers with lamina scheme of $45^\circ/-45^\circ/\ldots$ using different sampling points N ($h/l = 0.1$)

N	$[45^\circ/-45^\circ]$	$e\%$	$[45^\circ/-45^\circ/45^\circ]$	$e\%$	$[(45^\circ/-45^\circ)_2]$	$e\%$
5	0.0645598	−1.64	0.0898695	−1.37	0.0870414	−1.46
6	0.0651963	−0.67	0.0908178	−0.33	0.0880077	−0.36
7	0.0656576	0.04	0.0911396	0.03	0.0883568	0.03
8	0.0656408	0.01	0.0911178	0.005	0.0883337	0.005
9	0.0656339	0.0004	0.0911134	−0.0003	0.0883292	−0.0003
Exact [3]	0.0656341	—	0.0911137	—	0.0883295	—
M2D-11 [5]	0.0656171	−0.03	0.0910756	−0.04	0.0883003	−0.03

N	$[(45^\circ/-45^\circ)_2]/45^\circ$	$e\%$	$[(45^\circ/-45^\circ)_6]$	$e\%$	$[(45^\circ/-45^\circ)_6]/45^\circ$	$e\%$
5	0.0927712	−1.42	0.0939545	−1.46	0.0945072	−1.46
6	0.0938043	−0.32	0.0950290	−0.34	0.0955869	−0.33
7	0.0941368	0.03	0.0953784	0.03	0.0959344	0.03
8	0.0941125	0.004	0.0953528	0.004	0.0959087	0.004
9	0.0941083	−0.0003	0.0953484	−0.0003	0.0959044	−0.0003
Exact [3]	0.0941086	—	0.0953487	—	0.0959047	—
M2D-11 [5]	0.0940783	−0.03	0.0953201	−0.03	0.0958829	−0.02

Table 2
Fundamental frequency parameters $\bar{\omega}$ of strongly thick SS plates composed of different layer numbers with lamina scheme of 45°/−45°/… using different sampling points N

	$[45°/-45°]$	$[45°/-45°/45°]$	$[45°/-45°]_2$	$[45°/-45°]_2/45°$	$[45°/-45°]_6$	$[45°/-45°]_{20}/45°$
$h/l = 0.3$						
6	0.461664	0.488649	0.498429	0.512590	0.535290	0.541466
7	0.462278	0.489207	0.498940	0.513058	0.535691	0.541861
8	0.462173	0.489136	0.498871	0.512994	0.535623	0.541792
9	0.462165	0.489129	0.498865	0.512988	0.535619	0.541787
Exact [3]	0.462166	0.489130	0.498865	0.512989	0.535619	0.541788
$h/l = 0.4$						
6	0.713670	0.720231	0.728322	0.741146	0.772058	0.781670
7	0.714257	0.720840	0.728906	0.741694	0.772505	0.782100
8	0.714123	0.720744	0.728822	0.741621	0.772435	0.782029
9	0.714116	0.720737	0.728815	0.741614	0.772430	0.782024
Exact [3]	0.714117	0.720738	0.728816	0.741615	0.772431	0.782025

Table 3
Fundamental frequency parameters $\bar{\omega}$ of CC plates composed of different layer numbers with lamina scheme of 45°/−45°/… using different sampling points N ($h/l = 0.1$)

N	$[45°/-45°]$	e%	$[45°/-45°/45°]$	e%	$[(45°/-45°)_2]$	e%
5	0.13281	1.22	0.14926	−0.32	0.15167	0.13
6	0.13230	0.83	0.14935	−0.26	0.15108	−0.26
7	0.13128	0.05	0.14975	0.01	0.15145	−0.01
8	0.13122	0.01	0.14973	−0.01	0.15144	−0.02
9	0.13121	—	0.14974	—	0.15147	—

N	$[(45°/-45°)_2]/45°$	e%	$[(45°/-45°)_6]$	e%	$[(45°/-45°)_6]/45°$	e%
5	0.15719	0.16	0.16306	0.55	0.16350	0.54
6	0.15656	−0.24	0.16217	0.00	0.16263	0.01
7	0.15694	0.00	0.16235	0.11	0.16281	0.12
8	0.15692	−0.01	0.16224	0.04	0.16271	0.06
9	0.15694	—	0.16217	—	0.16262	—

Table 4
First six frequency parameters $\bar{\omega}$ of a CC thick plate with lamina scheme of 0°/45°/0°/45° using different sampling points N ($h/l = 0.25$)

N	Mode					
	1	2	3	4	5	6
5	0.61005	1.45887	1.69545	—	—	—
6	0.61265	1.21816	1.68354	—	—	—
7	0.61279	1.23480	1.68468	1.87384	—	—
8	0.61277	1.23358	1.68429	1.93185	2.52044	—
9	0.61270	1.23367	1.68433	1.91960	2.57509	2.66468
10	0.61269	1.23350	1.68432	1.92079	2.87911	2.62189
11	0.61267	1.23351	1.68432	1.92019	2.87871	2.62779
12	0.61267	1.23348	1.68432	1.92022	2.87875	2.62573
13	0.61267	1.23348	1.68432	1.92020	2.87873	2.62589

Note: '—' denotes result not obtainable.

lamina scheme of $0^\circ/45^\circ/0^\circ/45^\circ$. In these two tables, all results for frequency parameters are given in five digits. Relative deviation of the results from that obtained using $N = 9$ are also tabulated in Table 3. Comparisons show that at least three digits remain the same for the results of $N = 7$ and 9 with a maximal relative deviation of 0.12%. When $N = 8$, this value is only 0.06%, with indication that it is adequate to set results of $N = 9$ as the comparison standard. Table 4 delivers that SSDQM is also highly efficient for determining higher-order frequency parameters of thick laminates. When $N = 12$ and 13, at least five digits remain the same for the first five frequencies, while for the sixth frequency, four digits are the same. It should be pointed out that the third frequency corresponds not to the three-half-wave mode but to the second order of the one-half-wave mode. From physical sense, a given N is adequate for predicting the frequencies of small number of half waves, but it is not necessarily the case for large number of half waves. This is obviously illustrated in Table 4.

Table 5 gives the first six frequency parameters for CC laminates with different aspect ratios. The lamina schemes are of $50^\circ/30^\circ/50^\circ/30^\circ$ (Scheme A) and $50^\circ/-30^\circ/50^\circ/-30^\circ$ (Scheme B), and sampling point number is taken as $N = 13$. Numerical results indicate that, for the same aspect ratio and layer number, lamina scheme poses a significant effect on vibration behavior of the plates. For plate of $h/l = 0.1$, the first two frequencies for Scheme A are larger than that for Scheme B. This situation is converse for the next four frequencies. But for thick plates of $h/l = 0.25$ and 0.4, only the fundamental frequency for Scheme A is larger than that for Scheme B.

Finally, effects of ply angle on vibration behavior of angle-ply laminates are investigated. Figs. 2 and 3 depicted the variation of first three frequency parameters $\bar{\omega}$ of SS and CC plates ($s = 0.1$), respectively. Figs. 2(a) and 3(a) are for antisymmetric lamina scheme of $\theta/-\theta$, while Figs. 2(b) and 3(b) for symmetric

Table 5
First six frequency parameters $\bar{\omega}$ of CC plates of different aspect ratios with lamina schemes of $[50^\circ/30^\circ]_2$: *Scheme A*; and $[50^\circ/-30^\circ]_2$: *Scheme B* ($N = 13$)

Mode	$h/l = 0.1$		$h/l = 0.25$		$h/l = 0.4$	
	Scheme A	Scheme B	Scheme A	Scheme B	Scheme A	Scheme B
1	0.1792	0.1654	0.5780	0.5406	0.9842	0.9394
2	0.3840	0.3556	1.0918	1.1041	1.7169	1.8896
3	0.4521	0.5787	1.1758	1.7345	1.9596	2.9283
4	0.6235	0.8143	1.8089	2.2607	2.6341	3.1491
5	0.8741	0.9901	2.1222	2.3882	3.0038	3.4995
6	0.8901	1.0591	2.2763	2.8447	3.2588	3.9926

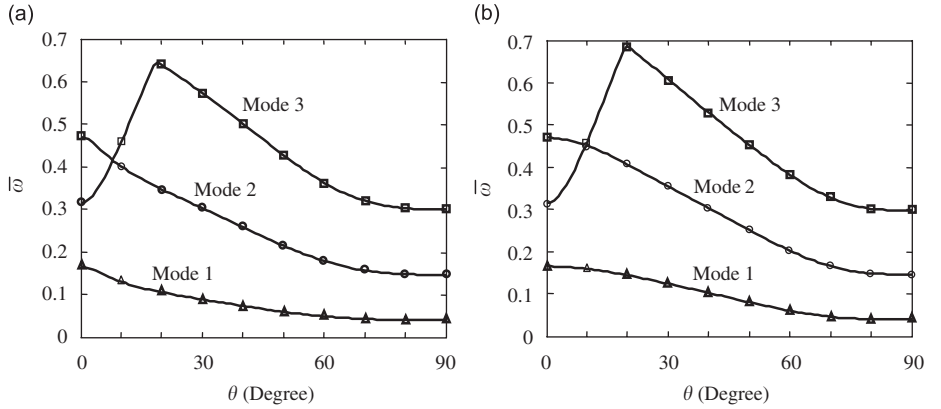

Fig. 2. Variation of first three frequency parameters $\bar{\omega}$ of SS plate versus the ply angle θ for antisymmetric ($\theta/-\theta$) and symmetric ($\theta/-\theta/\theta$) lamina schemes ($h/l = 0.1$, $N = 9$).

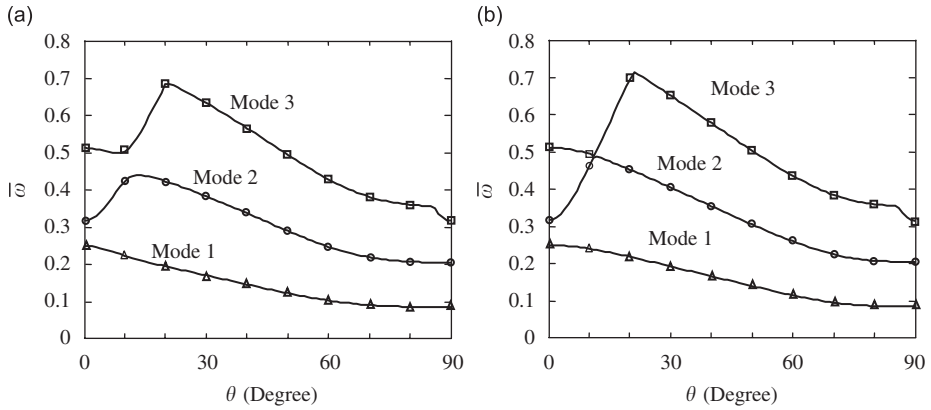

Fig. 3. Variation of first three frequency parameters $\bar{\omega}$ of CC plate versus the ply angle θ for antisymmetric $((\theta/-\theta))$ and symmetric $(\theta/-\theta/\theta)$ lamina schemes $(h/l = 0.1, N = 9)$.

scheme of $\theta/-\theta/\theta$. It is observed from the figures that the fundamental frequency parameter $\bar{\omega}$ decreases monotonically as the ply angle increases from 0° to 90°, $\bar{\omega}$ for the second vibration mode increases first and then decreases, and for the third vibration mode, $\bar{\omega}$ decreases first, next increases and then decreases again. Frequency parameters decrease very slowly as θ increases in the vicinity of 90° for all modes in consideration except for the third vibration mode of CC plate. It is seen from Fig. 3 that $\bar{\omega}$ for the third mode experiences a sharp jump-down when θ goes through 85°. Investigation of mode shapes indicates that there is mode shape switching in the second mode for each case at the kink points of about $\theta = 9.5^\circ$ for SS plates and $\theta = 12^\circ$ for CC plates. Similarly, there are two kink points in the third mode of SS plates, indicating that the mode shape switches twice as θ increases from 0° to 90°. In fact, the critical point of jump-down on the $\bar{\omega} - \theta$ curves for the third mode of CC plate is also a kink point where mode shape switching occurs. Based on the above analysis, special concerns are suggested to be drawn about the possible mode shape switching due to fiber orientations when designing anisotropic composite laminates.

4. Conclusions

Free vibration of anisotropic angle-ply laminates in cylindrical bending is studied via the newly developed state-space-based differential quadrature method (SSDQM). The analysis is directly based on the basic equations of 3D elasticity, which discards the displacement and stress approximations along plate thickness direction, making the current method suitable for laminates with arbitrary thickness. Meanwhile, the present problem is approximately solved along the in-plane direction using the differential quadrature technique. The present method is not limited to angle-ply laminates, but it can be applicable to problems of laminates with arbitrary anisotropy, for which the state space formulation has been established by Tarn [18].

The application of differential quadrature removes the difficulties encountered by the conventional state space approach, which is confined to simply supported edges. Although only the laminates with clamped edges are considered, the present method can also deal with free edges in a similar way to the authors' previous work for laminated cantilever beams [11,12]. Semi-analytical results for fully clamped laminates, especially for strongly thick plates, are presented and expected to serve as benchmarks for future numerical analyses.

Acknowledgments

This work was supported by the National Natural Science Foundation of China (No. 10432030), by China Postdoctoral Science Foundation (No. 20060401071), and by the Program for New Century Excellent Talents in University of China (NCET-05-0510).

Appendix A

$$c_1 = Q_{11} - Q_{13}^2/Q_{33}, \quad c_3 = Q_{12} - Q_{13}Q_{23}/Q_{33}, \quad c_4 = -Q_{13}/Q_{33}, \quad c_5 = -Q_{23}/Q_{33},$$
$$c_6 = Q_{66} - Q_{36}^2/Q_{33}, \quad c_7 = Q_{44}/d, \quad c_8 = -Q_{45}/d, \quad c_9 = Q_{55}/d, \quad c_{10} = 1/Q_{33},$$
$$b_1 = Q_{16} - Q_{13}Q_{36}/Q_{33}, \quad b_2 = Q_{26} - Q_{23}Q_{36}/Q_{33}, \quad b_3 = -Q_{36}/Q_{33},$$

where $d = Q_{44}Q_{55} - Q_{45}^2$, and Q_{ij} are determined by the stiffness constants and fiber orientation θ as referenced in Ref. [19].

References

[1] N.J. Pagano, Exact solutions for composite laminates in cylindrical bending, *Journal of Composite Materials* 3 (1969) 398–411.
[2] N.J. Pagano, Influence of shear coupling in cylindrical bending of anisotropic laminates, *Journal of Composite Materials* 4 (1970) 330–343.
[3] W.Q. Chen, K.Y. Lee, Three-dimensional exact analysis of angle-ply laminates in cylindrical bending with interfacial damage via state-space method, *Composite Structures* 64 (2004) 275–283.
[4] X.P. Shu, K.P. Soldatos, Cylindrical bending of angle-ply laminates subjected to different sets of edge boundary conditions, *International Journal of Solids and Structures* 37 (2000) 4289–4307.
[5] A. Messina, Two generalized higher order theories in free vibration studies of multi-layered plates, *Journal of Sound and Vibration* 242 (2001) 125–150.
[6] A. Messina, K.P. Soldatos, A general vibration model of angle-ply laminated plates that accounts for the continuity of interlaminar stresses, *International Journal of Solids and Structures* 39 (2002) 617–635.
[7] R. Bellman, J. Casti, Differential quadrature and long-term integration, *Journal of Mathematical Analysis and Applications* 34 (1971) 235–238.
[8] R. Bellman, B.G. Kashef, J. Casti, Differential quadrature: a technique for the rapid solution of nonlinear partial differential equations, *Journal of Computational Physics* 10 (1972) 40–52.
[9] C.W. Bert, M. Malik, Differential quadrature method in computational mechanics: a review, *Applied Mechanics Reviews* 49 (1996) 1–28.
[10] C. Shu, *Differential Quadrature and its Application in Engineering*, Springer, London, 2000.
[11] W.Q. Chen, C.F. Lv, Z.G. Bian, Elasticity solution for free vibration of laminated beams, *Composite Structures* 62 (2003) 75–82.
[12] W.Q. Chen, C.F. Lv, Z.G. Bian, Free vibration analysis of generally laminated beams via state-space-based differential quadrature, *Composite Structures* 63 (2004) 417–425.
[13] W.Q. Chen, K.Y. Lee, On free vibration of cross-ply laminates in cylindrical bending, *Journal of Sound and Vibration* 273 (2004) 667–676.
[14] C. Shu, B.E. Richards, Application of generalized differential quadrature to solve two-dimensional incompressible Navier–Stokes equations, *International Journal for Numerical Methods in Fluids* 15 (1992) 791–798.
[15] A.N. Sherbourne, M.D. Pandey, Differential quadrature method in the buckling analysis of beams and composite plates, *Computers and Structures* 40 (1991) 903–913.
[16] R.J. Nagem, J.H. Williams, Dynamic analysis of large space structures using transfer matrices and joint coupling matrices, *Mechanics of Structures and Machines* 17 (1989) 349–371.
[17] C.F. Lü, Y.Y. Lee, C.W. Lim, W.Q. Chen, Free vibration of long-span continuous rectangular Kirchoff plates with internal rigid line supports, *Journal of Sound and Vibration* 297 (2006) 351–364.
[18] J.Q. Tarn, A state space formalism for anisotropic elasticity. Part I: Rectilinear anisotropy, *International Journal of Solids and Structures* 39 (2002) 5143–5155.
[19] J.R. Vinson, R.L. Sierakowski, *The Behavior of Structures Composed of Composite Materials*, Kluwer, London, 2002.